

The Influences of Water Vapor/Hydrogen Ratio, Gas-Flow Rate and Antimony on the Surface Oxidation of Trip Steels

Youjong Kwon[†], Jingxi Zhu¹, Il-Ryong Sohn², and Seetharaman Sridhar¹

^{3rd} floor Shinan Build, 945-19 Daechi-2dong, Gangnam-gu, Seoul, 135-845, Korea
previously, Carnegie Mellon University

¹Carnegie Mellon University, Department of Materials Science and Engineering,
5000 Forbes avenue, Pittsburgh, PA, 15213, USA

²POSCO Technical Research Labs, Gumho-dong, Gwangyang-Si, Jeonnam, 545-090, Korea

(Received October 14, 2009; No Revision; Accepted December 19, 2011)

In the current paper, we are reporting the results from an investigation of the surface and sub-surface oxidation of a TRIP steel containing 2 wt.% Mn and 0.5 wt.% Al with and without 0.03 wt.% Sb. The oxidizing conditions in the gas were successively varied in terms of the linear gas flow-rate and dew-point, from conditions where gas-phase mass transport limited conditions prevailed, to those where solid state processes became the rate determining conditions. It was found, that at sufficient low oxidizing conditions (defined as flow-rate/dew-point), the metal surfaces were clear of any external oxides, and as the oxidizing conditions were increased, Mn- and Si- oxide nodules formed along with magnetite. As the oxidizing conditions were increased further, a dense magnetite layer was present. The limits of the various regions were experimentally quantified and a proposed hypothesis for their occurrences is presented. No obvious effect of Sb was noted in this micro-structural research of the oxides that results from the various conditions investigated in this study.

Keywords : oxidation, TRIP, annealing, dew point, Sb

1. Introduction

The transformation included plasticity (TRIP) effect is useful for improving mechanical properties of automotive steel, primarily the ductility and strength. The phase components present in TRIP steel microstructure are ferrite, bainite and retained austenite, and this is obtained by subjecting the steel to a specially tailored annealing process.¹⁾

During deformation, the retained austenite phase enables high formability, and is transformed to martensite, which results in the ultra high strength. A typical chemical composition of TRIP steel is in the range of 0.1 to 0.2 wt.% C, 1.0 to 2.2 wt.% Si, and 1.0 to 3.0 wt.% Mn.¹⁾ With the aforementioned excellent mechanical properties, TRIP steel is an excellent candidate material for automotive parts.

One of the most pertinent issues, however, for the manufacturing of automotive parts that are exposed to the environment, is coatability in an in-line galvanizing process;

and this can be problematic for TRIP steels since selective surface oxidation can occur by the reactive alloying additions Mn, Si and/or Al. When reactive alloying elements are annealed in-line before immersion in the zinc bath during hot-dip galvanizing, the elements produce surface oxides on which the coating alloy may not readily wet and this can result in uncoated regions, which are called "bare spots".²⁾

Studies have been carried out on the fundamental kinetics of TRIP steel oxidation. As shown by Gong *et al.*³⁾, the internal oxides under equilibrium conditions were analyzed at N₂+10%H₂ atmosphere with +3 °C dew point. Three different kinds of oxide particles and thin film were found on the surface: 200-230 nm size single crystal MnO, crystalline 30-60 nm size xMnO·SiO₂ (1≤x≤4), amorphous α-xMnO·SiO₂ (0<x<0.9) oxide particles and 30 nm xMnO·SiO₂ (1<x<2) oxide film. Below 4 μm of the surface, oxidation particle and net were found.

Researches have also reported,^{2),4)} the transition from internal to external oxidation in TRIP steels in an Ar+5%H₂ atmosphere with various dew points by thermogravimetric technique. Baum *et al.*²⁾ elucidated the decarburiza-

[†] Corresponding author: youjong.kwon@samsung.com

tion as well as oxidation phenomenon. Oxidation was internal dominant and independent with decarburization. The rate of oxidation was followed by a parabolic oxidation law, and affected by dew point. The decarburization rate was slightly lower than the predicted rates based on carbon diffusion.

Zhang et al.⁴⁾ investigated the effect of alloying element additions (Si, P and Sb), and identified grain boundaries as important diffusion paths for Si and Mn. However the oxidation of TRIP surface during the annealing process is still not completely understood. The flow conditions are not known and the oxidizing gas species (water molecules in the gas) are of such low content that gas phases mass transport is rate controlling. The times for oxidation are short enough and mass changes small enough (as a result of the slow oxidation kinetics) that thermogravimetric analysis, which often involves long heating and cooling times and requires sufficiently measurable mass change, is not completely applicable.

In this study, surface oxidation of TRIP steel was elucidated after exposing the sample surface to a variety of dew points and gas flow rates in a gold-image furnace with the capability of heating and cooling at the rates fast enough to simulate the annealing process of industry. The TRIP chemistry investigated was 1.5 wt.% Si, 2.0 wt.% Mn, 0.5 wt.% Al and 0.2 wt.% C with and without the addition of 300 ppm Sb.

2. Experimental

2.1 Materials

The material for the experiment was manufactured by POSCO.¹⁾ The size of the samples investigated in this study was 4x4x1.6 mm and they were cut from a cold rolled steel sheet. For each experimental case, both kinds of samples, listed in Table 1, with and without Sb were used. The samples were polished to remove any pre-existing surface oxide and finally cleaned in ethanol.

2.2 Experimental method

The oxidation experiments were performed in the hot stage attached to a Confocal Scanning Laser Microscopy

Table 1. sample chemistries

Sample	C	Si	Mn	P	S	Al	Sb
#6	0.2	1.5	2.0	0.02	0.002	0.5	-
#10	0.2	1.5	2.0	0.02	0.002	0.5	0.03

(CSLM). Samples were placed in a sample holder inside 13.2 mm dia. quartz tube, which is installed in the hot stage. The quartz tube ensures that a linear gas flow is present which can be quantified, when analyzing the influence of gas phase mass transport. A dew point measurement was made continuously at the outlet to establish the H₂O gas pressure. Fig. 1 shows the CSLM, quartz tube and dew-point monitor.

The temperature profile based on the provided information from POSCO, is shown in Fig. 2. This profile was programmed in the CSLM temperature controller to simulate the annealing process, and the same profile was applied to every experiment.

Table 2 shows the experimental condition matrix with various dew point, gas flow rate and analytical methods. As can be seen, the matrix includes the 2 aforementioned sample chemistries, 5 different dew points and 4 different levels gas flow rates. The properties of gas flow were Ar+5%H₂ gas with various dew points and gas flow rate.

The dew point of gas flow was -50, -40, -30, -20 and -10 °C, which were 4.0, 13, 38, 100 and 260 Pa of H₂O gas partial pressure respectively. The gas flow rate was maintained at 400 ml/min (corresponding to a linear flow rate of 29.2 cm/min) through a quartz tube within the hot stage. The results reported in this section were those obtained from the SEM-EDS analysis of the surfaces and the cross-sections in the samples, and the XRD analysis of the surfaces.

To elucidate the effect of gas flow rate on the oxidation of TRIP steels, four different gas flow rate were used. The gas flow rates were 50, 200, 400 and 600 ml/min, which correspond to linear flow rates of 37, 150, 290 and 440 cm/min respectively. The dew point was maintained

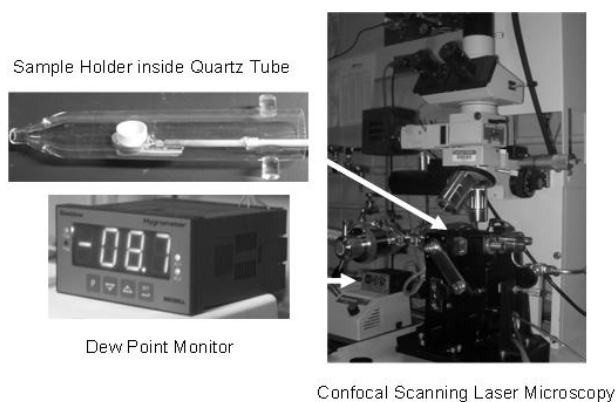


Fig. 1. Experimental apparatus.

1) POSCO Technical Research Labs., 699, Gumho-dong, Gwangyang-si, Jeonnam, 545-090, Korea

Table 2. Experimental condition and analysis

(i.e. gas composition : Ar+5%H₂)

Dew point		-50 °C		-40 °C		-30 °C		-20 °C		-10 °C	
Sample		#6	#10	#6	#10	#6	#10	#6	#10	#6	#10
Flow Rate (ml/min)	600					XRD SEM	XRD SEM				
	400	XRD SEM	XRD SEM	XRD SEM AES TEM	XRD SEM AES	XRD SEM					
	200					XRD SEM	XRD SEM				
	50					XRD SEM	XRD SEM				

Table 3. Experimental results of SEM-EDS, TEM and XRD

(i.e. *italic: TEM analysis*)

Dew point		-50 °C		-40 °C		-30 °C		-20 °C		-10 °C	
Sample		#6	#10	#6	#10	#6	#10	#6	#10	#6	#10
Flow Rate (ml/min)	600					Fe ₃ O ₄	Fe ₃ O ₄				
	400	Fe	Fe	Mn-Si-oxide <i>Si-oxide</i> <i>Mn</i>	Mn-Si-Oxide	Fe ₃ O ₄					
	200					Fe ₃ O ₄	Fe ₃ O ₄				
	50					Fe	Fe Si-oxide				

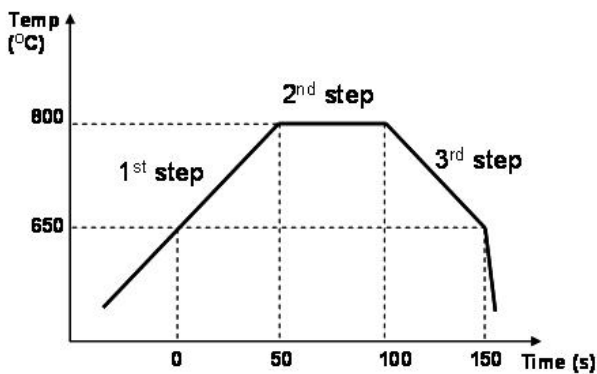


Fig. 2. Time-Temperature profile.

at -30 °C, which were 38 Pa of H₂O gas partial pressure.

After the oxidation experiments, SEM-EDS analysis was performed on the surfaces and cross-sections for evaluation of the morphology, thickness and chemistry of the oxides. In addition, XRD analysis was carried out to identify the structure of the major oxides present on the surface. In some cases, AES and TEM analysis were also

carried out to elucidate the oxide structures.

3. Results & discussion

3.1 Effect of Dew-Point & Flow-Rate

When the dew-point and/or flow-rate was very low, no major oxidation was found on the surface. As increasing dew-point and flow-rate, Mn-Si-oxide or Si-oxide was detected by SEM-EDS analysis, however, from the TEM analysis, the Mn-Si-oxide were revealed as Si-oxide and Metallic Mn; it shows the possibility of Mn reduction by Si-oxidation. When high dew-point and/or flow-rate, the Fe-oxide are covered the surface. The detailed analytical results are shown in Table 3, and described in Fig. 3 with modified Ellingham diagram.

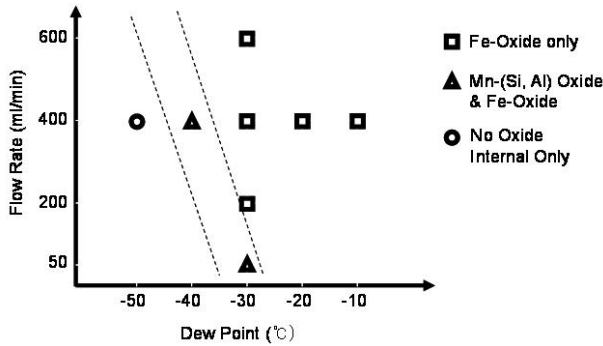
The modified Ellingham diagram shows the trends of oxide stability in the various oxidation conditions applied in this study, as shown in Fig. 3(b). It shows that Mn and Si oxide are stable in entire dew-point and temperature range, and Fe oxide are selectively stable depending on the dew-point and temperature, especially magnetite (Fe₃O₄)

has the highest stability temperature among Fe oxides. In other words, when the dew-point is sufficiently low, only Mn and Si oxidation is possible, but as the dew-point is increased, Fe oxides become stable and are expected to form a continuous layer in which magnetite is the most stable oxide.

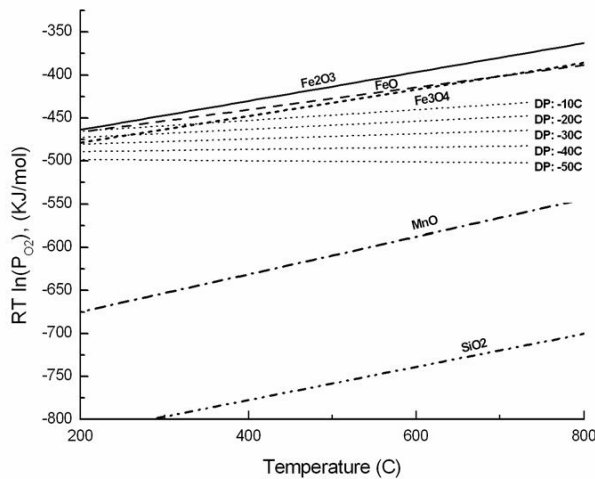
3.2 Oxidation Process with Heating, Isothermal and Cooling

Based on the analytical results of SEM-EDS, XRD and TEM shown in Table 3, the overall oxidation process depending on the dew-point and gas flow-rate can be elucidated. In Fig. 4, it is described the very low dew-points and/or flow-rates conditions, as shown in Fig. 3(circle). No-oxidation takes place, during heating, isothermal and cooling step, which is described 1st, 2nd and 3rd step in Figs. 2 and 4(a). This can be confirmed by inspection of Fig. 4(b).

In Fig. 5, the medium dew-point and flow-rate are described corresponding to the triangle points shown in Fig. 3, Mn and Fe oxidizes during the heating step as discussed in the previous section, but are reduced during the isothermal step, during which Si oxidation takes place. The



(a) The experimental results

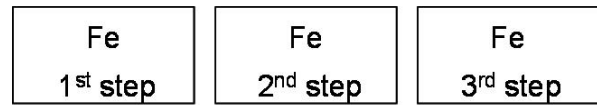


(b) Thermodynamic calculations (DP : dew-point)

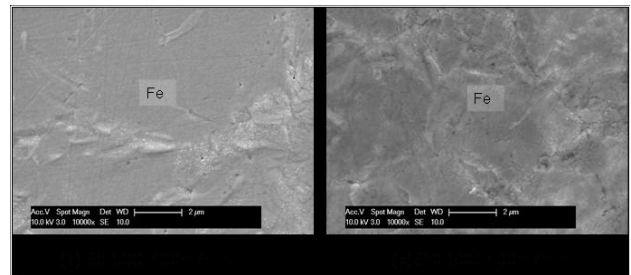
Fig. 3. The effect of flow rate and dew-point on surface oxidation.

TEM analysis result of Mn reduction and Si oxidation was shown in Table 3. In cooling step, a small amount of Fe oxidation and no Mn-oxidation can take place because of fast cooling rate. The Fe-oxide layer is composed primarily of magnetite and this is in agreement with the prediction that was discussed in section 3.1. The results of oxidation are shown in Fig. 5(b).

A high dew-point and flow-rate makes thick Fe-oxide only, as shown in Figs. 3(rectangular) and 6(b). During heating and cooling step, the Fe is oxidized at a fast rate, and reduced somewhat during isothermal step. The round shape of Fe₃O₄ could be the result of reduction, by hydrogen during this step. Hence the shape and thickness of Fe-oxides are presumed to be determined by the rates and amounts of oxidation and reduction.

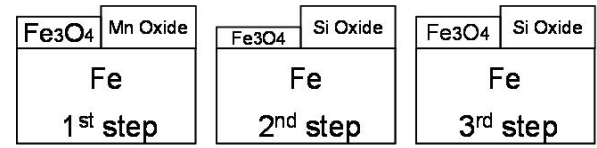


(a) Schematic oxidation

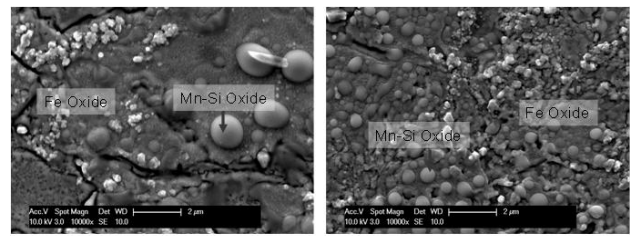


(b) Experimental results

Fig. 4. overall oxidation process at very low dew-point and flow-rate.



(a) Schematic oxidation

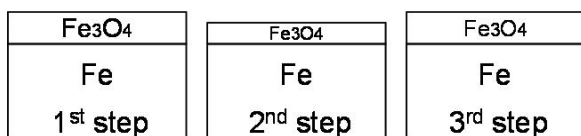


(c) #6-40C-400ml/min

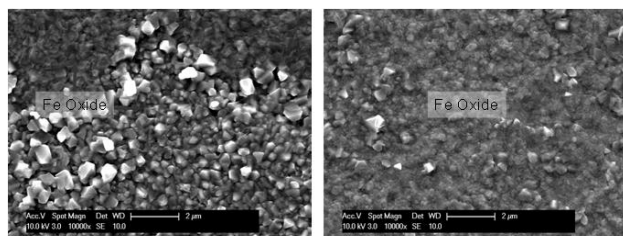
(d) #10-40C-400ml/min

(b) Experimental results

Fig. 5. overall oxidation process at medium dew-point and flow-rate.



(a) Schematic oxidation



(e) #6-30C-400ml/min

(f) #10-30C-400ml/min

(b) Experimental results

Fig. 6. overall oxidation process at high dew-point and flow-rate.

4. Summary

TRIP steel sample containing 0.5 wt.% C, 2.0 wt.% Mn, 1.5 wt.% Si, 0.5 wt.% Al with and without 300 ppm Sb was used to investigate the effect of $\text{H}_2\text{O}/\text{H}_2$ ratio, gas flow rate and antimony on the oxidation in simulated annealing process.

1) As the $\text{H}_2\text{O}/\text{H}_2$ ratio and/or flow-rate were increased, the thickness and chemical composition of oxide layer on the surface was changed, from no oxidation, to Mn-(Si, Al)-oxide & Fe_3O_4 , to Fe-oxides only.

2) It is proposed that the gas flow-rate and $\text{H}_2\text{O}/\text{H}_2$ ratio in the gas determined the flux of oxygen to the surface,

and the flux has an important role on the oxidation on the surface. When the flux of oxygen is lower than 2×10^{-9} mole/ $\text{cm}^2 \cdot \text{s}$, no oxidation was found. When the flux is higher than 5×10^{-9} mole/ $\text{cm}^2 \cdot \text{s}$, only Fe-oxide was found without Mn- or Si- oxide. And when the flux is between 2×10^{-9} and 5×10^{-9} mole/ $\text{cm}^2 \cdot \text{s}$, Fe-oxide and Mn-(Si, Al)-oxide coexisted.

3) The effect of Sb is limited by insufficient oxidation time. In the case of -30°C dew-point and 50 ml/min flow-rate, there was Fe-oxide and Mn-Si oxide on the surface of sample #6, and Si-oxide only on sample #10, as shown in Table 3. At the other dew-points and flow-rates, effects of Sb are found to be absent.

Acknowledgments

Financial support for this work from POSCO is acknowledged.

References

1. T. L. Baum, R. J. Fruehan, and S. Sridhar, *Metall. Trans. B*, **38**, 287 (2007).
2. S. Dionne, B. Voyzelle, E. Essadiqi, O. Dremailova, E. Baril, J. R. McDermid, and F. Goodwin, *Proc. Int. Conf. on Advanced High Strength Sheet Steels for Automotive Applications*, p. 405, AIST, Colorado (2004).
3. Y. F. Gong, H. S. Kim, and B. C. De Cooman, *ISIJ Int.*, **49**, 557 (2009).
4. Z. T. Zhang, I. R. Sohn, F. S. Pettit, G. H. Meier, and S. Sridhar, POSCO report (2008).